

<https://doi.org/10.1038/s43247-024-01268-z>

Summer heatwaves on the Baltic Sea seabed contribute to oxygen deficiency in shallow areas

Check for updates

Kseniia Safonova¹, H. E. Markus Meier¹✉ & Matthias Gröger¹

Since the early 1980ies, the shallow and brackish Baltic Sea, located in northern Europe, has warmed fastest of all the world's coastal seas. Hence, the total heat exposure during marine heatwaves increased in frequency and duration, which may have a major impact on the marine ecosystem. We found that marine heatwaves, using two different, commonly used definitions, occurred everywhere on the sea surface since the early 1990s. Periods with sea surface temperatures larger than 20 °C lasting longer than 10 days were particularly numerous in the shallow coastal zone of the southern and eastern Baltic Sea. Furthermore, summer marine heatwaves that reached the seabed mainly occurred in water depths of less than 20 m, where they led to a decrease in oxygen concentration. Since the early 1990s, a positive trend in the expansion of marine heatwaves has been observed on the seabed. The increasing number of marine heatwaves increases the risk of hypoxia events in the coastal zone.

Global average, sea and land surface temperature in 2001–2020 was about 1 °C higher than 1850–1900¹. However, the intensity of the warming is not evenly distributed across the different regions of the earth. Long-term observations from the Finnish archipelago (Storfjärden) in the northern Baltic Sea (Fig. 1) indicate that in the period from 1927 to 2020, sea surface and sea floor temperatures have increased by 1.8 and 1.3 °C, respectively². A pronounced warming, in particular since the early 1980s, is also reported from the outer edge of the archipelago and the deeper areas in the Baltic Sea, based on monitoring data as well as model-based reconstructions since 1850^{3–8}. Furthermore, future warming of the Baltic Sea is projected to be greater than the global average^{9,10}. Possible reasons are the land enclosure and a limited water exchange with the world ocean, as well as a permanent stratification due to excess freshwater supply from land. In the northern, seasonally ice-covered Baltic Sea, the warming of the water body is accelerated by the declining sea ice and the subsequent reduction in sea surface albedo¹⁰. This feedback mechanism is particularly pronounced in the Arctic region, which also affects the northern Baltic Sea. Therefore, the conditions in the Baltic Sea offer the opportunity to study the consequences of global warming on the marine ecosystem before they can be detected in other coastal seas around the world¹¹.

One consequence of global warming is the increase in terrestrial and marine heatwaves (MHWs)¹². MHWs, according to a widely used definition, are temperature anomalies for a period of five or more days that exceed the difference between the 90th percentile and the climatological mean for any day of the year¹³. If this criterion is fulfilled, the event is referred to as a

MHW Class I. If, on the other hand, the temperature anomaly exceeds the difference between the 90th percentile and the climatological mean twice, it is a MHW Class II, and so on. In this study, we focus on MHWs during the summer (June to September) lasting for at least 10 consecutive days with two fixed baseline periods, i.e., 1970–1993 and 1993–2020.

Another definition of MHWs is based on a seasonally fixed threshold for water temperature^{9,14}. For instance, we investigate periods with sea surface temperatures (SSTs) larger than 20 °C lasting longer than 10 days. For both definitions, the number and duration of MHWs will change if either the mean or the shape of the temperature probability distribution or both change. For the interpretation of results, the choice of the fixed baseline period is important^{2,15}. Alternatively, a shifting baseline might be used if the focus lies on dynamical processes rather than on global warming¹⁵, an approach that is not applied in this study.

During the past century, MHWs have become more frequent and more extended worldwide^{13,16,17}. Using the Hobday et al.¹³ approach (the first of the approaches explained above), Oliver et al.¹⁶ found an increase in global MHW average frequency and duration from 1925 to 2016 by 34% and 17%, respectively. These changes result in a 54% increase in annual MHW days globally and were mainly attributed to rising mean water temperatures. Since 2000, there have been several devastating MHWs with considerable societal and environmental impact such as the events in summer 2003^{18,19}, 2010²⁰ and 2023²¹, and the number of MHWs is projected to increase even further, on average by a factor of 16 and 41 for global warming of 1.5 and 3.5 °C relative to preindustrial levels, respectively¹⁷.

¹Department of Physical Oceanography and Instrumentation, Leibniz Institute for Baltic Sea Research Warnemünde, Rostock, Germany.

✉ e-mail: markus.meier@io-warnemuende.de

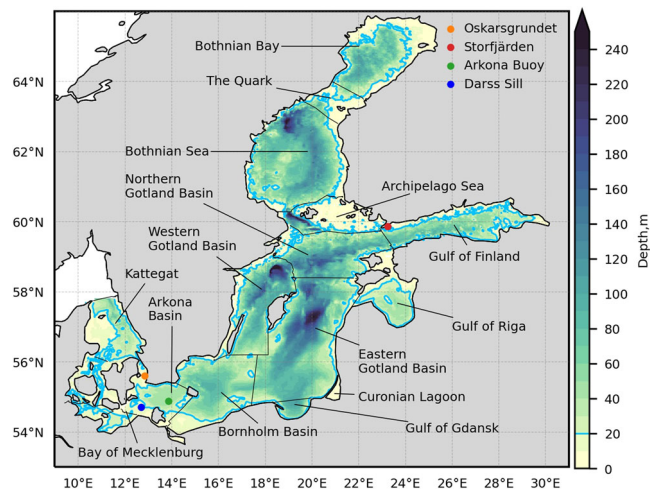


Fig. 1 | Bottom topography and locations of four permanent measurement stations. Shown are water depths (in m) and the locations of the Darss Sill Mast, the Arkona Buoy, as well as the stations in Oskarsgrundet and Storfjärden². The central Baltic Sea consists of the Eastern, Northern and Western Gotland Basin as well as the Bornholm Basin. In this study, the coastal zone is defined by the area with a water depth ≤ 20 m. The 20 m isobath is shown in light blue.

Apart from the aforementioned global assessments, knowledge about MHWs and their impact on regional seas like the Baltic and on shallow water ecosystems is still limited. Suursaar^{22,23} investigated the impact of the MHWs in summer 2014 and summer 2021 on the temperature variability in the Gulf of Finland, located in the northeastern Baltic Sea (Fig. 1). Goebeler et al.² found MHWs on the seabed in the entrance of the Gulf of Finland (Storfjärden, see Fig. 1) in each of the seasons 2016–2020, with intensities and durations exceeding previous records. As annual maximum temperatures in the Baltic Sea have increased more than mean temperatures²⁴ and MHWs tend to last much longer than heatwaves over land, i.e. up to weeks and months^{13,17}, they can have a greater impact on the marine ecosystem than the slower increase in mean temperature. In summer 2018, a MHW in the Finnish archipelago resulted in elevated outgassing of CO_2 and CH_4 , likely due to high respiration in the 21 °C bottom waters²⁵. According to Humborg et al.²⁵, these fluxes may be as large as maximum emission rates found in arctic and boreal lakes and wetlands.

Elevated temperatures are not the only threat for coastal seas like the Baltic Sea. Since the 1950s, the Baltic Sea has been suffering from an increasing lack of oxygen due to excess nutrient inputs from land in combination with a permanent haline stratification that impedes the natural oxygenation of the seabed in offshore regions^{26–31}. In addition, hypoxia in the coastal zone has also increased, probably exacerbated by global warming³². Conley et al.³² identified 115 sites that have experienced hypoxia during the period 1955–2009, with the Baltic Sea coastal zone containing over 20% of all known sites worldwide at the time of their study. This result was derived from monitored profiles with hypoxic conditions, which is problematic due to the limited number of measurements in space and time. Therefore, the observations do neither allow a comprehensive assessment of the area at risk nor to derive the relationship between MHWs and the concentration of dissolved oxygen.

In this study, the impact of MHWs on bottom oxygen concentrations is investigated. Higher water temperatures cause lower oxygen solubility³³. Furthermore, an increased thermal stratification during summer MHWs reduces the vertical transport of oxygen³⁴. Higher water temperatures also lead to a faster remineralisation of organic material and thus to a consumption of oxygen, especially in the sediment^{35,36}. Drivers of MHWs at the surface and at the seabed are different. While MHWs at the surface of a stratified marginal sea are mainly caused by meteorological conditions³⁴, deeper layers will only experience MHWs if, in addition to the atmospheric prerequisites, heat is transported vertically or horizontally below the

pycnocline. During 1982–2016, the seasonal thermocline and the perennial halocline have strengthened offshore in most of the Baltic Sea sub-basins³⁷. The strengthening of the halocline is explained by a systematical freshening of the upper layer and by an increase in salinity in the sub-halocline deep layer, likely caused by an increased lateral import of saltier water from the North Sea^{8,38}. These results are confirmed for the Bothnian Sea, in which a decrease in surface oxygen flux into the warming surface layer and a decrease in oxygen flux into the deep layer due to a strengthening of the halocline have been observed since the 1950s³⁹. The latter is a consequence of the overall freshening of the Baltic Sea surface layer on multi-decadal timescale⁴⁰. In the coastal zone with water depths less than 20 m, however, there is potential that the vertical stratification is dissolved by wind-induced mixing. In this case, the heat flux can reach the seabed during a MHW.

In order to shed light on the aforementioned multiple processes specific to shallow waters, we have studied the spatial and temporal temperature variability of the Baltic Sea with focus on MHWs. For this analysis, two ocean reanalysis datasets covering the periods 1970–1999⁴¹ (henceforth REA1) and 1993–2020^{42,43} (henceforth REA2) have been used. The two, above-mentioned definitions of a MHW (see also Methods) were compared. The study goes beyond previous approaches, as it focused on three-dimensional reanalysis datasets and not exclusively on satellite²³ or single station data². We investigated how summer MHWs affect bottom water oxygen concentrations, including the effects of reduced solubility of oxygen in seawater as well as changing vertical stratification.

We found that seasonal mean surface and bottom water temperatures of the two available reanalysis datasets agree well during the overlapping period (1993–1999). Summer MHWs at the seabed, defined as events with a bottom water temperature ≥ 17 °C lasting longer than 10 consecutive days, mainly occur in coastal waters with a water depth less than 20 m. Annual maximum MHW extents slightly differ between REA1 and REA2, which makes the detection of long-term trends problematic. We therefore recommend the creation of a longer, physically consistent reanalysis. Despite this uncertainty, annual maximum extents of summer MHWs on the seabed have shown, independently of the definition of MHWs, statistically significant, positive trends since 1993. Furthermore, we found that summer MHWs on the seabed of the shallow coastal zone cause a decrease in oxygen concentration due to the lower solubility. On average MHWs have locally been up to 10 °C warmer than during normal conditions without MHWs. Therefore, MHWs will very likely contribute more to hypoxia in the coastal zone in a future climate than in the current climate, with probably considerable impact on the marine ecosystem.

Results

Evaluation and comparison of reanalyses

The two reanalyses, REA1 and REA2, are evaluated with independent, high temporal resolution measurements at four permanent stations located mainly in shallow waters (see Fig. 1 for locations). We focus on daily surface and bottom water temperatures and near-bottom oxygen concentrations. The agreement in summer water temperature between reanalysis data and independent measurements at these permanent stations is generally relatively good, with absolute mean biases < 1 K and root mean square errors (RMSEs) < 5 K (Table 1, Fig. 2). At the station Storfjärden, located in the entrance to the Gulf of Finland (Fig. 1), greater discrepancies in bottom water temperatures are found than at the other stations because the closest water grid points in REA1 and REA2 are twice shallower than the observed depth at the monitoring site. Neither of the two datasets, REA1 and REA2, can be described as better fit to the measurements.

For near-bottom oxygen concentrations, the agreement between available observations at the Darss Sill Mast and Arkona Buoy and reanalysis data (REA2) is satisfactory (Supplementary Fig. 1, Supplementary Table 1). At the Arkona Buoy, we find absolute mean biases < 1 mL L⁻¹ and RMSEs < 1.5 mL L⁻¹. Correspondingly, we find at the Darss Sill Mast absolute mean biases < 1.5 mL L⁻¹ and RMSEs < 4 mL L⁻¹. The agreement at the Darss Sill Mast is worse than at the Arkona Buoy because the variability

Table 1 | Daily mean surface and bottom water temperatures at selected stations

	Storfjärden		Oskargrundet		Arkona Buoy		Darss Sill	
	surface	bottom	surface	bottom	surface	bottom	surface	bottom
Reanalysis	REA1	REA2	REA1	REA2	REA2	REA2	REA1	REA2
Location (lat, lon)	59.859167, 23.259722	1970–2020	55.5999, 12.8474	1983–1999	54.883333, 13.866667	2002–2020	54.7, 12.7	1995–2020
Period	1970–2020	1970–2020	1983–1999	1983–1999	2002–2020	2006–2020	1995–2020	1994–2020
Station depth [m]	2	29	2	43	2	43	2	19
REA depth [m]	1.5	13.5	1.5	46.5	1.5	46.5	1.5	19.5
N	3660	3416	1574	716	2033	1721	242	2558
Daily temperatures								
ME [°C]	-0.5	0.6	-0.1	0.8	-0.1	-1.0	-1.2	1.1
RMSE [°C]	3.6	2.6	1.2	1.4	0.5	4.5	5.2	3.9
R	0.81	0.89	0.90	0.95	0.96	0.83	0.61	0.79
Climatological daily 90th percentile of daily temperatures								
ME [°C]	0.6	0.2	0.1	-0.1	0.1	-0.6	0.1	0.2
RMSE [°C]	0.6	0.1	0.1	0.2	0.04	0.6	1.6	0.5
R	0.45	0.93	0.88	0.93	0.94	0.58	-0.06	0.31

Comparison between daily measurements and reanalysis data of surface and bottom summer (June, July, August and September) temperatures at Storfjärden, Oskargrundet, Arkona Buoy and Darss Sill (for the locations see Fig. 1). Listed are location, period, water depth of measurements and reanalysis data (REA1, REA2) (in m). The same statistical parameters are calculated for climatological daily 90th percentiles.

N number of observations, ME mean bias, RMSE root mean square error, R correlation.

of bottom oxygen concentrations in the Danish straits is high relative to the Baltic Sea sub-basins.

Moreover, the seasonal mean values of SST, bottom water temperature, bottom oxygen concentration and bottom salinity of the two reanalysis datasets, REA1 and REA2, for the overlapping period 1993–1999 are well comparable in most parts of the model domain (Supplementary Figs. 2–5). The differences are generally smaller than natural fluctuations. Note, however, that bottom salinities between REA1 and REA2 slightly differ, indicating different results for saltwater inflows and vertical stratification (Supplementary Fig. 5). Furthermore, during 1993–1999 in REA1 slightly higher annual (0.3 °C) and summer mean (0.6 °C) temperatures on the seabed in the coastal zone (≤ 20 m) than in REA2 are found, while the agreement for the seabed of the entire Baltic Sea is better. For the entire Baltic Sea, differences in annual and summer mean bottom temperatures between REA1 and REA2 amount to -0.03 °C and -0.2 °C, respectively.

Beside water temperature, the number and duration of MHWs, defined as events with a SST ≥ 20 °C lasting longer than 10 consecutive days, are similar in REA1 and REA2 for each individual year in the 1993–1999 period (Supplementary Fig. 6). The same applies to MHWs on the seabed, defined as events with a bottom water temperature ≥ 17 °C lasting longer than 10 consecutive days (Supplementary Fig. 7). However, differences in MHWs in the coastal zone are found during all seasons and in the northern Baltic Sea during spring and summer (not shown). These differences could be explained by the large temporal variability in shallow waters, which is not determined by data assimilation, and by the use of different sea ice models in REA1 and REA2, which might particularly be relevant for the northern Baltic Sea. As a result, the annual maximum extents of summer MHWs at the seabed during the overlapping period 1993–1999 are slightly larger in REA1 than in REA2, while the MHW extents at the sea surface are not significantly different (not shown). Therefore, no reliable trends for the annual maximum extent of summer MHWs can be calculated from the combined REA1 and REA2 datasets for the entire period 1970–2020. Instead, trend analyses remain limited to the individual periods of the reanalyses or to long-term measurements at single stations such as those from Storfjärden².

The comparison between the two reanalyses, REA1 and REA2, shows that in the case of the fixed threshold approach, the mean annual maximum MHW extent in REA2 during 1993–2020 in the entire Baltic Sea and in areas with a water depth >20 m is statistically significantly larger compared to REA1 during 1970–1993. This increase is explained by the mean warming rates between 1970–1993 and 1993–2020 (Supplementary Table 2). In contrast, the differences in the spatially averaged number and duration of MHWs between REA1 and REA2 are only small. In the case of the Hobday et al.¹³ approach, the spatially averaged numbers and durations are almost unchanged between REA1 and REA2. The difference in mean annual maximum MHW extent between REA1 and REA2 is statistically not significant.

Number, duration and extent of MHWs

At the sea surface, the number and mean duration of summer MHWs in the period 1970–1993, defined as events with a SST ≥ 20 °C lasting more than 10 consecutive days, are larger along the southern and eastern coasts compared to the open sea (Fig. 3a, b). In particular in the Curonian Lagoon, in the Szczecin coastal waters, in Pärnu Bay, in the coastal waters between Saaremaa and Hiiumaa and the Estonian mainland, in the easternmost part of the Gulf of Finland, and in the Finnish Archipelago Sea, frequent and long-lasting MHWs are found. No MHW event has been recorded in the central Gotland Basin during the period 1970–1993, while in the coastal zone, the number of MHWs could be up to 35 in the hot-spot areas. These coastal MHWs lasted up to 70 days (Fig. 3b). During the warmer period 1993–2020, typical numbers of summer MHWs increased to 10 in the central Gotland Basin and remained up to 35 in hot-spot areas of the coastal zone such as the Curonian Lagoon and the Greifswald Bay (Fig. 3c). Summer MHWs lasted about 20–30 days in the central Gotland Basin and longer in the Curonian Lagoon and the Greifswald Bay (Fig. 3d). In some years, the annual

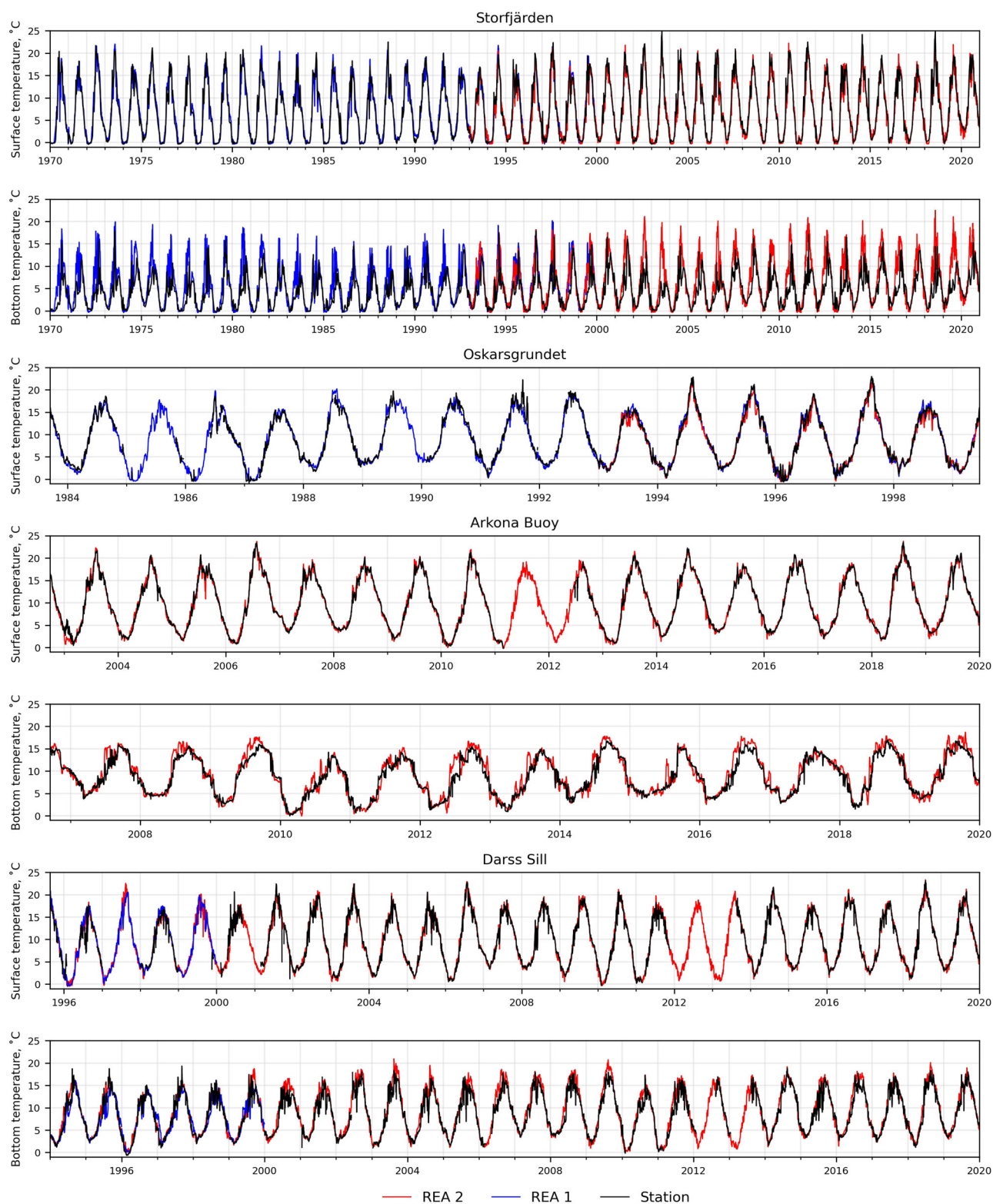


Fig. 2 | Daily water temperature measurements in coastal waters. Shown are observed and reanalysed (REA1 and REA2) daily mean sea surface and bottom water temperatures (in °C) from Storfjärden, Oskarsgrundet, Arkona Buoy, and Darss Sill (for the locations see Fig. 1).

maximum MHW extent in summer reached almost the entire surface of the Baltic Sea, for example in 2003, 2014 and 2018 (Fig. 3i). In neither of the two reanalyses did the annual maximum MHW extent at the sea surface change significantly (Supplementary Table 3).

Summer MHWs on the seabed, defined as events with a bottom temperature $\geq 17^\circ\text{C}$ lasting more than 10 consecutive days, are found

exclusively in shallow waters with a water depth $\leq 20\text{ m}$ (Fig. 3e, g). In the open sea with water depths greater than 40 m, such MHWs are not detected. Similar spatial distributions of MHW area, limited by the 20 m depth contour, are found for thresholds of 18, 19, and 20°C , with the number of MHWs consequently decreasing with increasing thresholds (Supplementary Fig. 8). Only during the period 1993–2020, the annual maximum extent

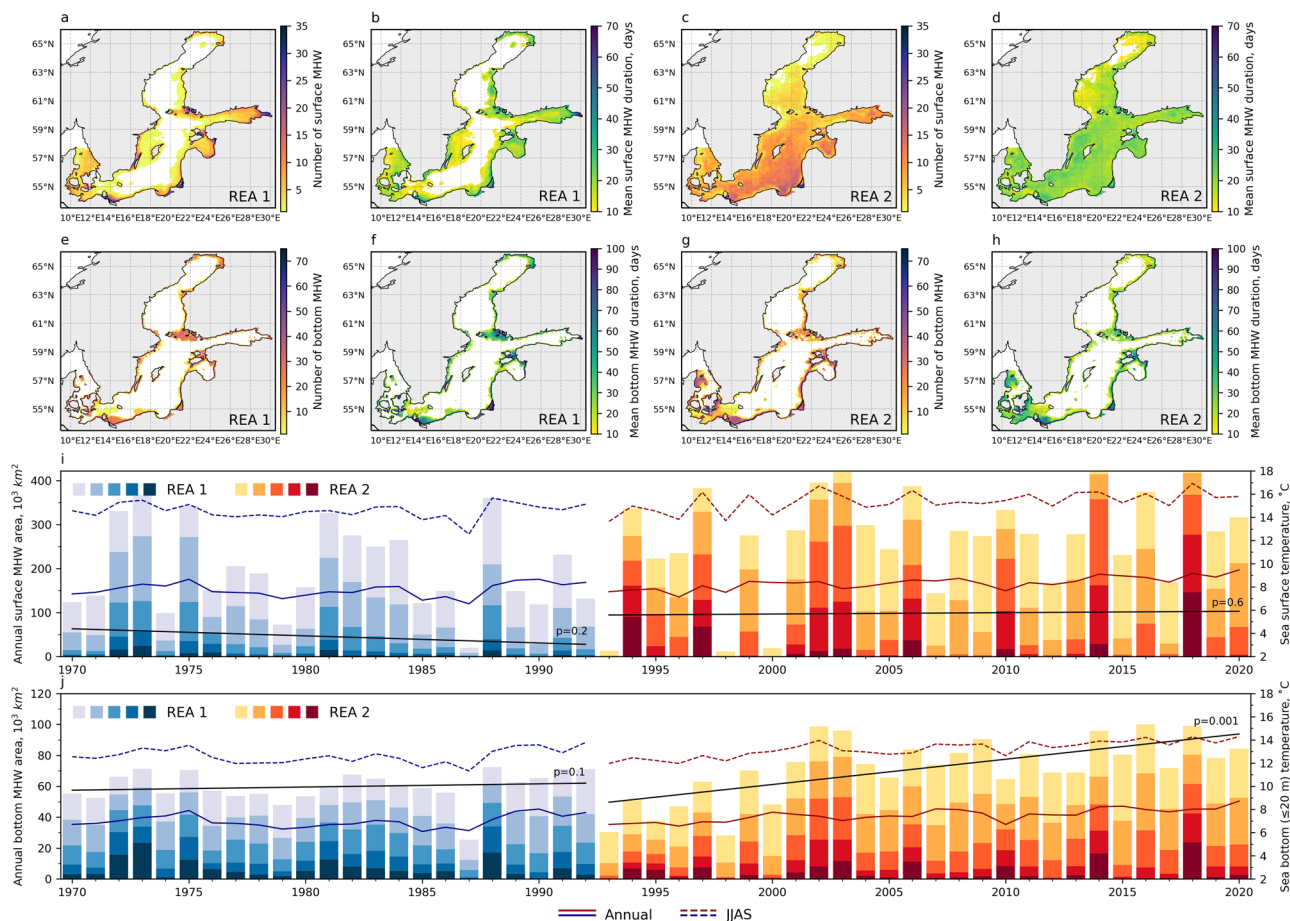


Fig. 3 | Characteristics of marine heatwaves in summer – approach I. Upper panels: Shown are the number of periods in summer (June to September) during 1970–1993 (a, e) and 1993–2020 (c, g) with a sea surface temperature (SST) $\geq 20^\circ\text{C}$ (a, c) or a bottom water temperature $\geq 17^\circ\text{C}$ (e, g) lasting for at least 10 consecutive days and their corresponding mean durations (in days) (b, d, f and h). Lower panels: Annual maximum extents of marine surface (i) and bottom (j) heatwaves in REA1 (bluish) and REA2 (reddish) (in 10^3 km^2). Shown are marine heatwaves with a SST

$\geq 18, 19, 20, 21, 22^\circ\text{C}$ (i) and with a bottom water temperature $\geq 17, 18, 19, 20, 21^\circ\text{C}$ (j) lasting for at least 10 consecutive days (from light to dark colours). In addition, annual (solid) and summer (June to September, dashed) mean sea surface and bottom water temperatures (in $^\circ\text{C}$) are shown (in blue and red). The latter for water depths $\leq 20\text{ m}$. Furthermore, trends in marine heatwave extent at the sea surface (SST $\geq 20^\circ\text{C}$) and at the seabed (bottom water temperature $\geq 17^\circ\text{C}$) in REA1 and REA2 are shown (in black).

of MHWs at the seabed shows a statistically significant positive trend based on the Mann–Kendall test (Fig. 3j). This trend amounts to $1.6 \times 10^3\text{ km}^2\text{ year}^{-1}$ (Supplementary Table 3).

At the sea surface, summer Class I MHWs, defined as water temperatures above the 90th percentile lasting more than 10 consecutive days, show a similar number of events in the open sea (~5–15 events over the period 1970–1993 or 1993–2020) as in the coastal zone (Fig. 4a, c). The longest mean duration of MHWs at the surface is found in the northern Baltic Sea (>30 days in the Bothnian Sea and Bothnian Bay) (Fig. 4b, d). Thus, the distribution of MHWs according to Hobday et al.¹³ differs as expected from the MHWs defined by fixed specific thresholds because the MHW definition by Hobday et al.¹³ accounts for the spatially variable mean temperatures.

However, on the seabed, summer MHWs of Class I show similar patterns to those of MHWs defined by a fixed threshold, with a greater number in the coastal zone (with a maximum of about 10 and 15 events in REA1 and REA2, respectively) compared to the open sea (<10 events) (Fig. 4e, g). In the open sea and coastal zone, these MHWs lasted more than 30 and 10–30 days on average, respectively (Fig. 4f, h). Only during the period 1993–2020 and only on the seabed did the annual maximum extent of Class I MHWs show a statistically significant positive trend according to the Mann–Kendall test (Fig. 4i, j). This trend amounts to $6.5 \times 10^3\text{ km}^2\text{ year}^{-1}$ (Supplementary Table 3), which is about four times larger than the trend in annual maximum

extent of MHWs defined by bottom temperatures $\geq 17^\circ\text{C}$ lasting more than 10 consecutive days.

As the intensity of MHWs, expressed by the class, increases, the number of MHWs consequently decreases (Fig. 5). Interestingly, for MHWs of classes II to IV in REA1 and REA2 and for MHWs of Class I in REA2, maxima in the number of events on the seabed are found in water depths $>20\text{ m}$, i.e., below the thermocline. The Class III and Class IV MHWs only exist in a depth range between 30 and 60 m, and the typical number of MHWs is only 1 event during either 1970–1993 or 1993–2020 (not shown). On the seabed of the deep areas of the Baltic Sea, neither Class III nor Class IV MHWs are found (Fig. 5).

Impact of summer MHWs on bottom oxygen concentrations

In the following, we analyse the summer bottom oxygen concentrations in the coastal zone under MHW and under normal conditions (without MHWs). During MHWs with bottom water temperatures $\geq 17^\circ\text{C}$ lasting at least 10 consecutive days, bottom oxygen concentrations in the coastal zone, characterised by water depths $\leq 20\text{ m}$, are lower than under normal conditions without MHWs (Fig. 6). Most of these differences up to -3 mL L^{-1} can be explained by the decreasing oxygen saturation concentration with increasing water temperature. Differences in mean bottom water temperatures between MHW and normal conditions (without MHWs) are considerable with values between 3 and 10°C (Supplementary Fig. 9). Indeed, there is a statistically significant correlation (MCC, see Method

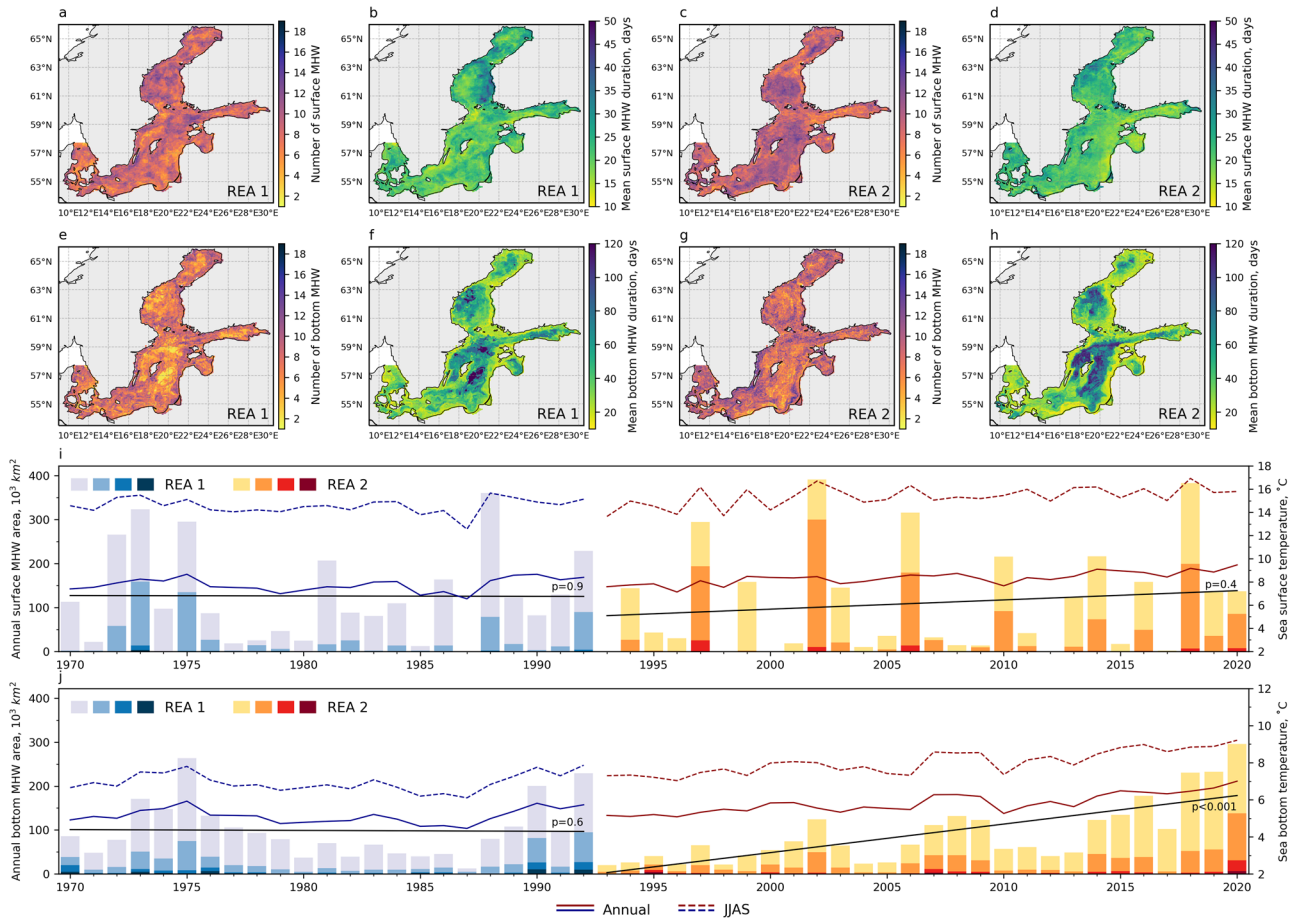


Fig. 4 | Characteristics of marine heatwaves in summer – approach II. Same as Fig. 3 but number and duration of summer (June–September) marine heatwaves (MHWs) of Class I in 1970–1993 (a, b, e and f) and 1993–2020 (c, d, g and h) according to Hobday et al.¹³. In the lower panels, the annual maximum extents of summer surface (i) and bottom (j) MHWs of Class I (light) to IV (dark) in REA1

(bluish) and REA2 (reddish) are shown. In addition, annual (solid) and summer (dashed) mean sea surface and bottom water temperatures (in °C) are shown (in blue and red). The latter for all water depths. Furthermore, trends in MHW Class I extent at the sea surface and at the seabed in REA1 and REA2 are shown (in black).

section) between low oxygen events with bottom oxygen concentrations $\leq 7 \text{ mL L}^{-1}$ and MHW events (Supplementary Fig. 10). The choice of the fixed threshold value is irrelevant for the oxygen differences shown in Fig. 6. However, the bottom area where MHWs occur in the coastal zone becomes smaller as the threshold value for water temperature increases (Supplementary Fig. 11).

However, the bottom oxygen concentration differences between MHW and normal conditions are not only attributed to the temperature-dependent changes in oxygen solubility. There are additional secondary effects from changes in stratification and temperature-dependent biological processes. These effects can be measured by the apparent oxygen utilisation (AOU), which is the difference between the oxygen saturation concentration and the oxygen concentration⁴⁴. In June and July, the AOU in the bottom waters of the coastal zone of all sub-basins is normally negative due to oxygen production by photosynthesis (Fig. 7, upper panels). This result is observed in both reanalyses for the period 1970–1993 (REA1) and 1993–2020 (REA2). However, in August and September, the AOU in coastal zone bottom waters becomes positive due to oxygen consumption, probably caused by amplified remineralisation in the sediments or reduced diffusive vertical oxygen fluxes to the bottom waters due to the summer thermocline.

In both reanalyses, AOU differences in the coastal zone between Class I MHWs¹³ and normal conditions (without MHWs) are relatively small, i.e., $<0.6 \text{ mL L}^{-1}$ (Fig. 7, lower panels), suggesting that the effect of processes other than the oxygen solubility that may alter bottom oxygen concentrations during MHWs is small.

In the open sea anomalous high AOU under Class I MHWs¹³ coincide with an intensified and shallower halocline reducing the oxygen flux to the bottom and supporting higher AOU. As summer MHWs are characterised by reduced wind speeds³⁴, mixing is reduced explaining increased stratification. The AOU differences are more pronounced in REA1 than in REA2 probably because of the different mixing parameterisations or atmospheric wind fields used.

Discussion

Previous studies on MHWs are based on either satellite or coarse-resolution climate model data. Thus, analyses are limited to the sea surface or are subject to the typically large uncertainties in model simulations. With the help of two reanalysis datasets from the shallow Baltic Sea, MHWs at the seabed could be analysed for the first time to our knowledge and their effects on the oxygen concentration at the bottom could be investigated.

Impact of MHWs on the marine ecosystem

It is well known that MHWs threaten marine ecosystems and biodiversity^{45–47}. Extreme MHWs might even cause mass mortality of vulnerable species. In the Mediterranean Sea, for example, impacts on growth, survival, fertility, migration and phenology of pelagic and benthic organisms, from phytoplankton to marine vegetation, invertebrates and vertebrates have been reported⁴⁵. Often problems arise for ecosystems when MHWs threaten critical foundation species such as corals, seagrasses, fucus and kelps.

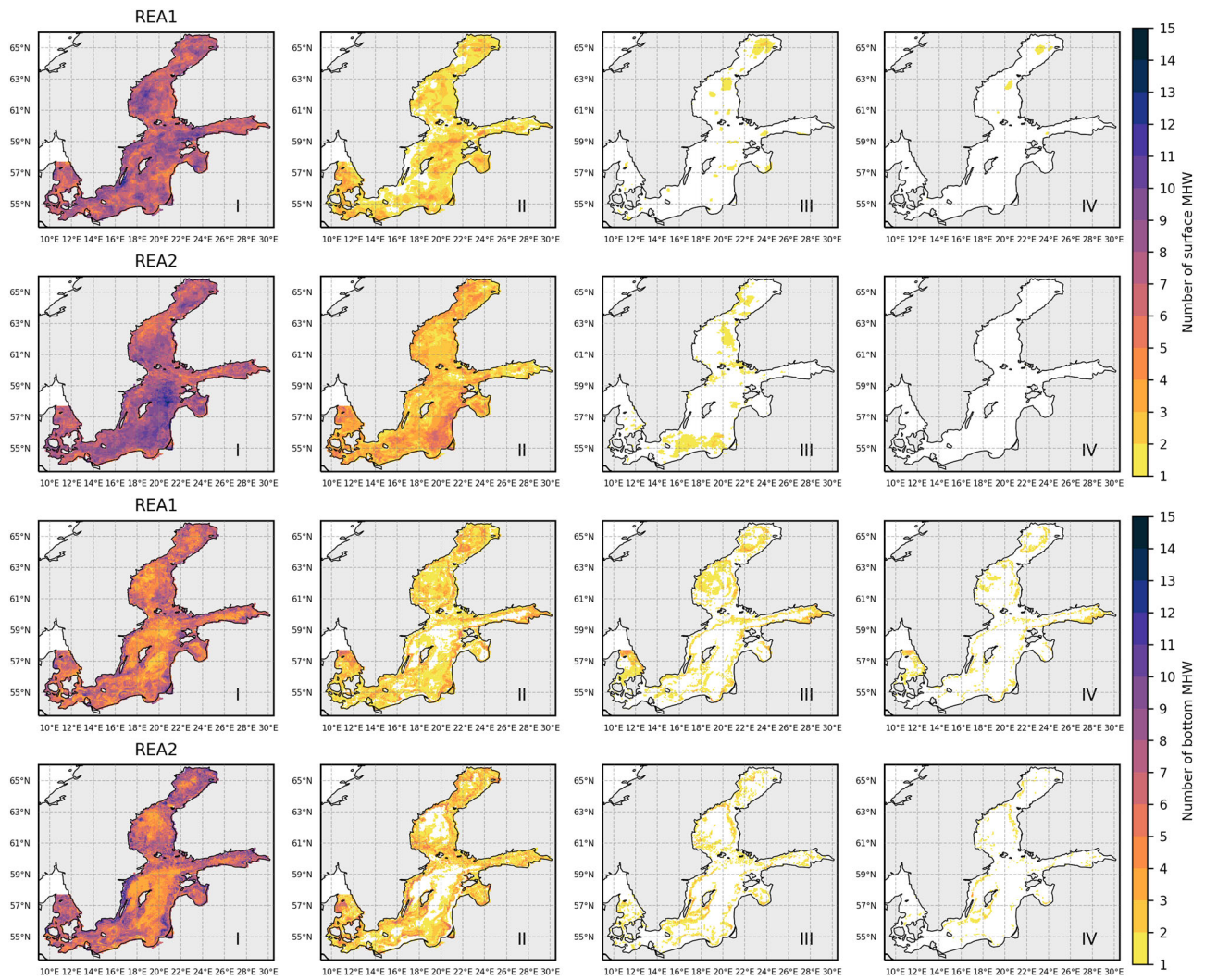


Fig. 5 | Marine heatwave classes in summer. Shown are numbers of summer (June–September) marine heatwaves (MHWs) of Class I to IV following Hobday et al.¹³. The upper and lower two rows of panels show surface and bottom MHWs for 1970–1993 and 1993–2020, respectively.

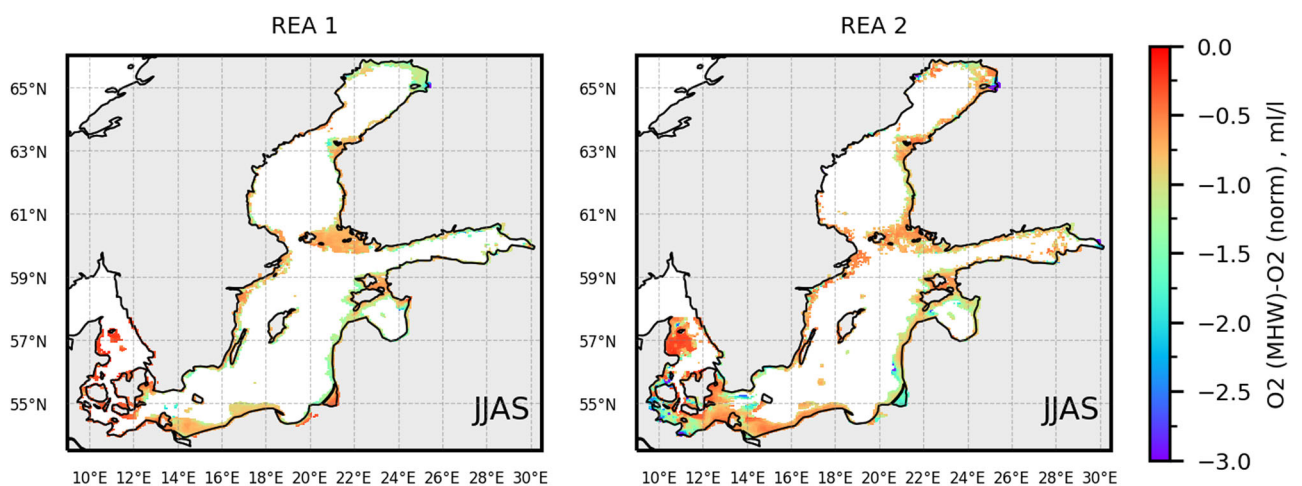


Fig. 6 | Bottom oxygen concentration changes during summer marine heatwaves. Shown are differences between bottom oxygen concentrations (in mL L^{-1}) during marine heatwaves (MHWs) with a bottom water temperature $\geq 17^\circ\text{C}$ lasting for at least 10 consecutive days and during normal conditions (without MHWs) in summer (June–September). Left panel: REA1 (1970–1993). Right panel: REA2 (1993–2020). Only statistically significant values are shown.

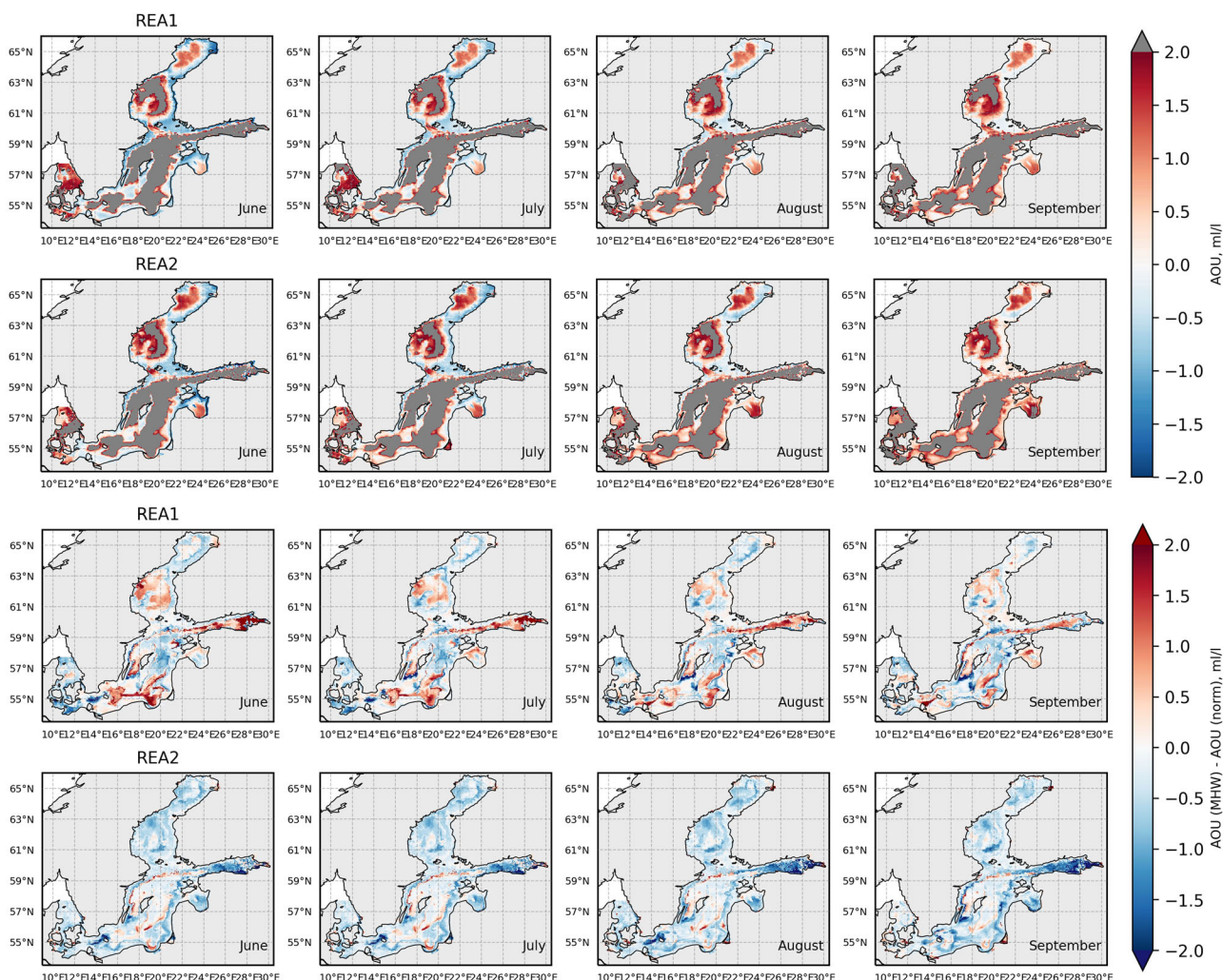


Fig. 7 | Apparent oxygen utilisation in summer. Monthly mean apparent oxygen utilisation (AOU, in mL L^{-1}) during 1970–1993 (REA1, first row) and 1993–2020 (REA2, second row). Shown is the difference between the oxygen saturation concentration and the oxygen concentration in the bottom water for June to September. In larger depths below the halocline, the bottom oxygen concentration is always

lower than the oxygen saturation concentration and AOU is positive (shown in grey). The third and fourth rows show the monthly AOU differences between marine heatwave (MHW) of Class I (Hobday et al.¹³) and normal conditions (in mL L^{-1}) during 1970–1993 (REA1, third row) and 1993–2020 (REA2, fourth row).

The Baltic Sea ecosystem is also threatened by MHW in many ways. First, due to the low salinity high temperatures together with excess nutrients, especially phosphorus, increase the risk of massive cyanobacterial blooms, which can increase oxygen consumption³⁷. Several field and modelling studies suggest that climate-induced temperature increase, together with increasing hypoxia and release of phosphorus from sediments⁴⁸, has promoted cyanobacterial blooms^{49–51}. However, the responses vary from species to species, and different environmental processes and food web interactions may control the abundance of cyanobacteria⁵². Second, the extent of anoxic areas is positively correlated with bottom temperature, indicating temperature-dependent remineralisation of organic matter³¹. Finally, there are many small lagoons and fjords in the Baltic Sea with limited water exchange with the open sea, which are often enriched with organic matter. Therefore, hypoxia is also increasingly occurring in coastal waters³².

As the frequency of summer MHWs at the seabed of the shallow coastal zone with water depths ≤ 20 m has increased since 1993 (this study) and as the frequency is expected to increase in the future due to global warming⁹, threats to the marine ecosystem will also increase. The identified high vulnerability of the coastal zone to oxygen depletion and heat stress associated with MHW events should be considered in future marine spatial planning and management of marine protected areas, either by reducing

ecosystem stressors other than climate warming or by designating areas with less warming than the large-scale average as protected areas (climate refuges)^{53–55}.

In the context of climate warming, it is often argued that low-trophic species can at least partially adapt to increased heat stress due to their higher reproductive rates^{56,57}. However, MHWs have long-lasting negative impacts on benthic organisms such as starfish⁵⁸. Furthermore, the decline in herring in the western Baltic Sea was related to rising winter temperatures followed by too-early peaks in spawning⁵⁹.

Definitions of marine heatwaves

As there is no definition of MHWs that suits all applications, we investigated two different definitions for summer MHWs, a fixed threshold approach¹⁴ and the approach by Hobday et al.¹³ with a fixed baseline. Amaya et al.¹⁵ argued that for multi-decadal changes in temperature the phrase ‘long-term temperature trends’ should be used. A ‘MHW’ would then be a short-term, extremely warm event relative to a shifting climatological reference period. However, if the application focusses on the impact of MHWs on biological organisms, fixed species-specific thermal thresholds related to physiological performance of organisms are more relevant than extremes defined relative to a fixed or shifting climatology¹⁴. Furthermore, in the case of historical data time series, the calculation of MHW based on fixed threshold values is easier

to implement and therefore of particular interest for impact assessments, as long-term time series of the background climate are usually lacking and statistical threshold values are therefore difficult to calculate or subject to great uncertainty.

For summer MHWs the two definitions, used in this study, gave similar results (Figs. 3 and 4, Supplementary Table 2), in particular for REA2 on the seabed. For MHWs on the seabed of the coastal zone with water depths ≤ 20 m, the mean water temperature exceeds approximately 13 °C (Supplementary Fig. 12) while the 90th percentile exceeds 17 °C (Supplementary Fig. 13). Hence, it is obvious that in this case both definitions are rather similar. However, the trend in annual maximum extent of MHWs in the Hobday et al. approach is about 4 times larger than the corresponding trend in the threshold approach.

Shortcomings due to horizontal resolution

In both reanalysis datasets, the bottom oxygen concentrations in the coastal zone are possibly overestimated in some places (Supplementary Fig. 14) because the horizontal grid resolution of 3.7 km is too coarse to correctly reflect the bathymetry and the associated residence times of the bottom water in small bays, fjords and lagoons. However, the reanalysis data from the coastal zone cannot be validated due to the lack of corresponding independent observations. An exception is the monitoring station in Storfjärden. Although today's environmental conditions may not be accurately represented, our results suggest drastic oxygen reduction rates under MHW presence in future climates and the emerging threat of coastal hypoxia.

Differences between reanalysis products

The reanalysis data, REA1 and REA2, differ not only in the spatially averaged water temperature because the time span of REA1 is earlier than that of REA2 and therefore colder. Furthermore, two different ocean circulation models, two different assimilation methods and different assimilated observation datasets were used in the reanalyses. The reader is referred to the Method section for details.

Although both reanalyses show similar overall results for SST and bottom water temperature in the open ocean during the overlap period 1993–1999 (Supplementary Figs. 2 and 3), and although the mean number, mean duration and mean annual maximum extent of MHWs are not statistically distinguishable when using the Hobday et al. approach (Supplementary Table 2), some differences between REA1 and REA2 are found.

For example, there are significant differences in SST (Supplementary Fig. 2) and bottom water temperature (Supplementary Fig. 3) in the coastal zone area, presumably because there are no measured profiles there and because natural variability is very high in the coastal zone. Furthermore, the models apparently include different parameterisations of vertical mixing. This would explain the differences in lateral saltwater transport and in vertical stratification, further affecting oxygen concentration (Supplementary Fig. 4) and salinity at the bottom (Supplementary Fig. 5).

Therefore, at least for the coastal zone, a merged dataset for the whole period 1970–2020 would not be homogeneous. Hence, our results indicate that there is a need for a physically consistent long reanalysis dataset for the analysis of MHWs.

Methods

Reanalysis data

As systematic studies of MHWs in the entire Baltic Sea, in particular below the sea surface, are lacking, we studied two reanalysis datasets by Liu et al.⁴¹ and by the Copernicus Marine Environmental Monitoring Service (CMEMS)^{42,43}. Liu et al.⁴² assimilated profiles of temperature, salinity, oxygen, nitrate, phosphate as well as ammonium concentrations at monitoring stations from the Swedish Ocean Archive (SHARK; <http://sharkweb.smhi.se>) using the RCO-SCOBI model^{60,61} and the Ensemble Optimal Interpolation (EnOI) method⁶². This reanalysis is limited to the period 1970–1999 and called REA1. The RCO-SCOBI model has a horizontal and vertical resolution of 3.7 km and 3 m (83 vertical levels), respectively.

The second reanalysis used is from CMEMS, called REA2. It covers the period 1993–2020 and used the NEMO-SCOBI model with a horizontal resolution of 3.7 km and 56 vertical levels, with layer thicknesses between 3 m close to the surface and 22 m at the bottom of the deepest part of the model domain, located in the Norwegian trench^{63,64}. REA2 assimilated SST observations from the Swedish Ice Service at the Swedish Meteorological and Hydrological Institute (SMHI) as well as in situ measurements for temperature and salinity from the ICES database⁴² and oxygen, nitrate, phosphate as well as ammonium concentrations from SHARK⁴³. For the assimilation, the Localised Singular Evolutive Interpolated Kalman (LSEIK) filter⁶⁵ was applied.

Hence, the two reanalyses, REA1 and REA2, are based upon different Baltic Sea models (though the spatial resolution is similar), different data assimilation methods and different observational datasets. While REA1 is solely based upon profile data from the Swedish monitoring programme, REA2 utilises additional temperature and salinity profiles from other national monitoring programmes and satellite data of SST and sea ice coverage.

Furthermore, we focused on SST and bottom temperature representing the temperature of the upper- and lowermost grid boxes, respectively. While the thicknesses of the surface grid boxes are identical in REA1 and REA2 (3 m), the thicknesses of the bottom grid boxes at greater depths differ, an issue contributing to the uncertainty in trends in MHWs of the bottom water only at greater depths.

Measurements at permanent stations

Four different independent datasets were used for the evaluation of REA1 and REA2. We aim to investigate whether the reanalyses are capable to resolve extreme temperatures at the sea surface and near the sea floor on the synoptic timescale that result in MHWs. The four stations are located in shallow waters (Fig. 1, Table 1). The measurement mast at Darss Sill and the buoy in the central Arkona Basin belong to the German national environmental monitoring programme operating since 1980 and 1995, respectively. The station Oskarsgrundet is located in the Öresund and belong to the Swedish national environmental monitoring programme. Finally, the longest available record since 1927 consists of the measurements in Storfjärden belonging to the Finnish Tvärminne Zoological Research station². For more details, the reader is referred to Table 1.

Marine heatwave definitions

Two approaches to calculate MHWs based upon daily mean data were used. While the model output of REA2 is daily, the snapshots of REA1 every second day were linearly interpolated. The first approach utilised absolute temperature thresholds ranging from 18 to 22 °C at the sea surface and from 17 to 21 °C at the seabed. MHWs were then defined as events with a water temperature exceeding the threshold temperature lasting for at least 10 consecutive days during the summer months June to September. From these data, the numbers of MHWs per grid cell during 1970–1993 and 1993–2020 were calculated for the REA1 and REA2 datasets, respectively. In Figs. 3 and 4, for the overlapping period 1993–1999 data from REA2 were used. From the MHW data per grid cell annual maximum areas were compiled and their temporal developments are compared with the area-averaged SST or with the area-averaged bottom temperature with water depths ≤ 20 m or for the entire seabed. From all MHW events during 1970–1993 and 1993–2020 a mean duration was calculated.

The second approach follows the classification by Hobday et al.^{13,66}. Instead of an absolute temperature threshold, a MHW Class I is defined as an event with a water temperature exceeding the 90th percentile of the temperature distribution of the specific calendar day for the periods 1970–1993 and 1993–2020 lasting for at least 10 consecutive days during the summer months June to September. Furthermore, a Class II MHW is defined as an event when the water temperature exceeds twice the difference between the 90th percentile and the mean of the specific summer day for the periods 1970–1993 and 1993–2020. Higher classes of MHWs were calculated accordingly. From the MHW events per grid cell, the mean duration and the annual maximum MHW area were derived.

Analysis strategy

As explained in the previous sub-section, for SST and bottom temperature, the frequency of summer MHWs, their mean duration, and their annual maximum extent were calculated for the periods 1970–1993 and 1993–2020. Their robustness against various temperature thresholds and classes following Hobday et al.¹³ was tested. In this study, we focussed on the effects of summer MHWs at the seabed on bottom oxygen concentrations. The summer season was defined as the period between June and September because during this period a seasonal thermocline prevails and bottom oxygen concentrations decline due to oxygen consumption with the risk of seasonal hypoxia. Following Carstensen et al.²⁷, we calculated the apparent oxygen utilisation (AOU) as the difference between the oxygen saturation concentration and the oxygen concentration. AOU at the seabed of the coastal zone is negative during spring and early summer due to photosynthesis of algae, while it is positive during late summer and autumn due to the remineralisation of dead organic material.

Furthermore, correlations between MHWs and bottom oxygen concentration minimum events were calculated. For this purpose, the time series of the parameters were converted into a binary form, with days when a MHW occurred as 1 and days without a MHW as 0. Low oxygen concentration events were defined as events when the oxygen concentration at the bottom drops to below 6, 7 or 8 mL L⁻¹ (Supplementary Fig. 14). The threshold for MHW events was 17 °C lasting for at least 10 days. The Matthew correlation coefficient (MCC) was calculated for the binary time series at each grid point. For binary variables, MCC is a special case of the Pearson correlation coefficient (PCC). MCC evaluates each category of the confusion matrix (true positives, false negatives, true negatives, and false positives) with respect to the other ones, proportionally both to the size of positive elements and the size of negative elements in the dataset^{67,68}.

Data availability

Water depth data depicted in Fig. 1 are publicly available from <https://www.io-warnemuende.de/topography-of-the-baltic-sea.html>. The reanalysis data by Liu et al.⁴¹ (REA1) are available from the Leibniz Institute for Baltic Sea Research Warnemünde (IOW) at the doi server <https://doi.io-warnemuende.de/10.12754/data-2023-0012> and the Copernicus (CMEMS) reanalysis data for the Baltic Sea (REA2) are available from <https://doi.org/10.48670/moi-00012> (oxygen concentration) and <https://doi.org/10.48670/moi-00013> (water temperature). Daily measurements from Storfjärden and Oskarsgrundet are available from <https://doi.org/10.5061/dryad.8cz8w9gtf> and <https://www.smhi.se/data/oceanografi/ladda-ner-oceanografiska-observationer#stationid=35067>, respectively. The Darss Sill Mast and the Arkona Buoy belong to the German MARNET monitoring network and data can be requested under https://www.bsh.de/EN/TOPICS/Monitoring_systems/MARNET_monitoring_network/_Module/Karussell/_documents/measuring_stations_baltic_sea_node.html.

Received: 12 March 2023; Accepted: 13 February 2024;

Published online: 28 February 2024

References

- IPCC. *Climate Change 2021: The Physical Science Basis. Contribution of Working Group I to the Sixth Assessment Report of the Intergovernmental Panel on Climate Change* 3949 (Cambridge Univ. Press, 2021).
- Goebeler, N., Norkko, A. & Norkko, J. Ninety years of coastal monitoring reveals baseline and extreme ocean temperatures are increasing off the Finnish coast. *Commun. Earth Environ.* **3**, 215 (2022).
- Fonselius, S. & Valderrama, J. One hundred years of hydrographic measurements in the Baltic Sea. *J. Sea Res.* **49**, 229–241 (2003).
- Belkin, I. M. Rapid warming of large marine ecosystems. *Prog. Oceanogr.* **81**, 207–213 (2009).
- Laakso, L. et al. 100 years of atmospheric and marine observations at the Finnish Utö Island in the Baltic Sea. *Ocean Sci.* **14**, 617–632 (2018).
- Kniebusch, M., Meier, H. E. M., Neumann, T. & Börgel, F. Temperature variability of the Baltic Sea since 1850 and attribution to atmospheric forcing variables. *J. Geophys. Res. Oceans* **124**, 4168–4187 (2019).
- Dutheil, C., Meier, H. E. M., Gröger, M. & Börgel, F. Understanding past and future sea surface temperature trends in the Baltic Sea. *Clim. Dyn.* **58**, 3021–3039 (2022).
- Dutheil, C., Meier, H. E. M., Gröger, M. & Börgel, F. Warming of Baltic Sea water masses since 1850. *Clim. Dyn.* **61**, 1311–1331 (2023).
- Meier, H. E. M. et al. Oceanographic regional climate projections for the Baltic Sea until 2100. *Earth Syst. Dyn.* **13**, 159–199 (2022).
- Meier, H. E. M. et al. Climate change in the Baltic Sea region: a summary. *Earth Syst. Dyn.* **13**, 457–593 (2022).
- Reusch, T. B. H. et al. The Baltic Sea as a time machine for the future coastal ocean. *Sci. Adv.* <https://doi.org/10.1126/sciadv.aar8195> (2018).
- Oliver, E. C. J. et al. Marine heatwaves. *Annu. Rev. Mar. Sci.* **13**, 313–342 (2021).
- Hobday, A. J. et al. Categorizing and naming marine heatwaves. *Oceanography* **31**, 162–173 (2018).
- Galli, G., Solidoro, C. & Lovato, T. Marine heat waves hazard 3D maps and the risk for low motility organisms in a warming Mediterranean sea. *Front. Mar. Sci.* <https://doi.org/10.3389/fmars.2017.00136> (2017).
- Amaya, D. J. et al. Marine heatwaves need clear definitions so coastal communities can adapt. *Nature* **616**, 29–32 (2023).
- Oliver, E. C. J. et al. Longer and more frequent marine heatwaves over the past century. *Nat. Commun.* **9**, 1324 (2018).
- Frölicher, T. L., Fischer, E. M. & Gruber, N. Marine heatwaves under global warming. *Nature* **560**, 360–364 (2018).
- García-Herrera, R., Díaz, J., Trigo, R. M., Luterbacher, J. & Fischer, E. M. A review of the European summer heat wave of 2003. *Crit. Rev. Environ. Sci. Technol.* **40**, 267–306 (2010).
- Olita, A. et al. Effects of the 2003 European heatwave on the Central Mediterranean Sea: surface fluxes and the dynamical response. *Ocean Sci.* **3**, 273–289 (2007).
- Barriopedro, D., Fischer, E. M., Luterbacher, J., Trigo, R. M. & Garcia-Herrera, R. The hot summer of 2010: redrawing the temperature record map of Europe. *Science* **332**, 220–224 (2011).
- Copernicus Marine Service. *The 2023 Northern Hemisphere Summer Marks Record-Breaking Oceanic Events* <https://marine.copernicus.eu/news/2023-northern-hemisphere-summer-record-breaking-oceanic-events> (2023).
- Suursaar, Ü. Combined impact of summer heat waves and coastal upwelling in the Baltic Sea. *Oceanologia* **62**, 511–524 (2020).
- Suursaar, Ü. Summer 2021 marine heat wave in the Gulf of Finland from the perspective of climate warming. *Est. J. Earth Sci.* **71**, 1–16 (2022).
- Gröger, M. et al. The Baltic Sea Model Intercomparison Project (BMIP) – a platform for model development, evaluation, and uncertainty assessment. *Geosci. Model Dev.* **15**, 8613–8638 (2022).
- Humborg, C. et al. High emissions of carbon dioxide and methane from the coastal Baltic Sea at the end of a summer heat wave. *Front. Mar. Sci.* <https://doi.org/10.3389/fmars.2019.00493> (2019).
- Conley, D. J. et al. Hypoxia-related processes in the Baltic Sea. *Environ. Sci. Technol.* **43**, 3412–3420 (2009).
- Carstensen, J., Andersen, J. H., Gustafsson, B. G. & Conley, D. J. Deoxygenation of the Baltic Sea during the last century. *Proc. Natl Acad. Sci. USA* **111**, 5628–5633 (2014).
- Gustafsson, B. G. et al. Reconstructing the development of Baltic Sea eutrophication 1850–2006. *Ambio* **41**, 534–548 (2012).
- Meier, H. E. M. et al. Disentangling the impact of nutrient load and climate changes on Baltic Sea hypoxia and eutrophication since 1850. *Clim. Dyn.* **53**, 1145–1166 (2019).

30. Almroth-Rosell, E. et al. A regime shift toward a more anoxic environment in a Eutrophic Sea in Northern Europe. *Front. Mar. Sci.* <https://doi.org/10.3389/fmars.2021.799936> (2021).
31. Krapf, K., Naumann, M., Dutheil, C. & Meier, H. E. M. Investigating hypoxic and euxinic area changes based on various datasets from the Baltic Sea. *Front. Mar. Sci.* <https://doi.org/10.3389/fmars.2022.823476> (2022).
32. Conley, D. J. et al. Hypoxia is increasing in the coastal zone of the Baltic Sea. *Environ. Sci. Technol.* **45**, 6777–6783 (2011).
33. Carpenter, J. H. New measurements of oxygen solubility in pure and natural water. *Limnol. Oceanogr.* **11**, 264–277 (1966).
34. Gröger, M., Dutheil, C., Börgel, F. & Meier, H. E. M. Drivers of marine heat waves in a stratified marginal sea. *Clim. Dyn.* <https://doi.org/10.1007/s00382-023-07062-5> (2024).
35. Meier, H. E. M., Väli, G., Naumann, M., Eilola, K. & Frauen, C. Recently accelerated oxygen consumption rates amplify deoxygenation in the Baltic Sea. *J. Geophys. Res. Oceans* **123**, 3227–3240 (2018).
36. Börgel, F. et al. Deoxygenation of the Baltic Sea during the last millennium. *Front. Mar. Sci.* <https://doi.org/10.3389/fmars.2023.1174039> (2023).
37. Liblik, T. & Lips, U. Stratification has strengthened in the Baltic Sea – an analysis of 35 years of observational data. *Front. Earth Sci.* <https://doi.org/10.3389/feart.2019.00174> (2019).
38. Barghorn, L., Meier, H. E. M. & Radtke, H. Changes in seasonality of saltwater inflows caused exceptional warming trends in the western Baltic Sea. *Geophys. Res. Lett.* **50**, e2023GL103853, <https://doi.org/10.1029/2023GL103853> (2023).
39. Polyakov, I. V. et al. Depletion of oxygen in the Bothnian Sea since the mid–1950s. *Front. Mar. Sci.* <https://doi.org/10.3389/fmars.2022.917879> (2022).
40. Meier, H. E. M. et al. Multidecadal climate variability dominated past trends in the water balance of the Baltic Sea watershed. *npj Clim. Atmos. Sci.* **6**, 58 (2023).
41. Liu, Y., Meier, H. E. M. & Eilola, K. Nutrient transports in the Baltic Sea – results from a 30-year physical–biogeochemical reanalysis. *Biogeosciences* **14**, 2113–2131 (2017).
42. Liu, Y. et al. Baltic Sea Production Centre BALTICSEA_REANALYSIS_PHY_003_011. 35pp (COPERNICUS Marine Environment Monitoring Service, 2019).
43. Axell, L. et al. Baltic Sea Production Centre BALTICSEA_REANALYSIS_BIO_003_012. 51pp (COPERNICUS Marine Environment Monitoring Service, Issue 2.5, 2019).
44. Garcia, H. E., Boyer, T. P., Levitus, S., Locarnini, R. A. & Antonov, J. On the variability of dissolved oxygen and apparent oxygen utilization content for the upper world ocean: 1955 to 1998. *Geophys. Res. Lett.* <https://doi.org/10.1029/2004GL022286> (2005).
45. Marbà, N., Jorda, G., Agusti, S., Girard, C. & Duarte, C. M. Footprints of climate change on Mediterranean Sea biota. *Front. Mar. Sci.* <https://doi.org/10.3389/fmars.2015.00056> (2015).
46. Frölicher, T. L. & Laufkötter, C. Emerging risks from marine heat waves. *Nat. Commun.* **9**, 650 (2018).
47. Smale, D. A. et al. Marine heatwaves threaten global biodiversity and the provision of ecosystem services. *Nat. Clim. Change* **9**, 306–312 (2019).
48. Vahtera, E. et al. Internal ecosystem feedbacks enhance nitrogen-fixing cyanobacteria blooms and complicate management in the Baltic Sea. *Ambio* **36**, 186–194 (2007).
49. Kahru, M., Elmgren, R., Kaiser, J., Wasmund, N. & Savchuk, O. Cyanobacterial blooms in the Baltic Sea: correlations with environmental factors. *Harmful Algae* **92**, 101739 (2020).
50. Neumann, T. et al. Extremes of temperature, oxygen and blooms in the Baltic Sea in a changing climate. *Ambio* **41**, 574–585 (2012).
51. Meier, H. E. M. et al. Future projections of record-breaking sea surface temperature and cyanobacteria bloom events in the Baltic Sea. *Ambio* **48**, 1362–1376 (2019).
52. Viitasalo, M. & Bonsdorff, E. Global climate change and the Baltic Sea ecosystem: direct and indirect effects on species, communities and ecosystem functioning. *Earth Syst. Dyn. Discuss* **2021**, 1–38 (2021).
53. Perry, D., Hammar, L., Linderholm, H. W. & Gullström, M. Spatial risk assessment of global change impacts on Swedish seagrass ecosystems. *PLoS ONE* **15**, e0225318 (2020).
54. Queirós, A. M. et al. Solutions for ecosystem-level protection of ocean systems under climate change. *Global Change Biol* **22**, 3927–3936 (2016).
55. Laikre, L. et al. Lack of recognition of genetic biodiversity: International policy and its implementation in Baltic Sea marine protected areas. *Ambio* **45**, 661–680 (2016).
56. Irwin, A. J., Finkel, Z. V., Müller-Karger, F. E. & Troccoli Ghinaglia, L. Phytoplankton adapt to changing ocean environments. *Proc. Natl Acad. Sci. USA* **112**, 5762–5766 (2015).
57. Schaum, C. E. et al. Adaptation of phytoplankton to a decade of experimental warming linked to increased photosynthesis. *Nat. Ecol. Evol.* **1**, 0094 (2017).
58. Wolf, F. *Extreme Events And Warming in the Baltic Sea: Relevance for Coastal Benthic Communities* (University of Kiel, 2022).
59. Polte, P. et al. Reduced reproductive success of western Baltic herring (*Clupea harengus*) as a response to warming winters. *Front. Mar. Sci.* <https://doi.org/10.3389/fmars.2021.589242> (2021).
60. Meier, H. E. M., Döscher, R. & Faxén, T. A multiprocessor coupled ice-ocean model for the Baltic Sea: application to salt inflow. *J. Geophys. Res. Oceans* **108**, 3273 (2003).
61. Eilola, K., Meier, H. E. M. & Almroth, E. On the dynamics of oxygen, phosphorus and cyanobacteria in the Baltic Sea; a model study. *J. Marine Syst.* **75**, 163–184 (2009).
62. Liu, Y., Meier, H. E. M. & Eilola, K. Improving the multiannual, high-resolution modelling of biogeochemical cycles in the Baltic Sea by using data assimilation. *Tellus A* **66**, 24908 (2014).
63. Pemberton, P. et al. Sea-ice evaluation of NEMO-Nordic 1.0: a NEMO-LIM3. 6-based ocean–sea-ice model setup for the North Sea and Baltic Sea. *Geosci. Model Dev.* **10**, 3105 (2017).
64. Hordoir, R. et al. Nemo-Nordic 1.0: a NEMO-based ocean model for the Baltic and North seas – research and operational applications. *Geosci. Model Dev.* **12**, 363–386 (2019).
65. Nerger, L., Hiller, W. & Schröter, J. A comparison of error subspace Kalman filters. *Tellus A* **57**, 715–735 (2005).
66. Hobday, A. J. et al. A hierarchical approach to defining marine heatwaves. *Prog. Oceanogr.* **141**, 227–238 (2016).
67. Chicco, D. & Jurman, G. The advantages of the Matthews correlation coefficient (MCC) over F1 score and accuracy in binary classification evaluation. *BMC Genom.* **21**, 6 (2020).
68. Chicco, D., Tötsch, N. & Jurman, G. The Matthews correlation coefficient (MCC) is more reliable than balanced accuracy, bookmaker informedness, and markedness in two-class confusion matrix evaluation. *BioData Mining* **14**, 13 (2021).

Acknowledgements

The presented research is part of the Baltic Earth programme (Earth System Science for the Baltic Sea region, see <http://baltic.earth>) and the new focus programme on Shallow Water Processes and Transitions to the Baltic Scale at the Leibniz Institute of Baltic Sea Research Warnemünde (IOW) (<https://www.io-warnemuende.de/stb-shallow-water-processes.html>). Furthermore, the study is a contribution to the BMBF funded project CoastalFutures (03F0911E). Measurements at Darss Sill and from the Arkona Buoy are part of the national environmental monitoring programme operated by the Leibniz Institute of Baltic Sea Research Warnemünde and financed by the Federal Maritime and Hydrographic Agency Hamburg and Rostock (BSH) (https://www.bsh.de/EN/DATA/Climate-and-Sea/Marine_environment_monitoring_network/marine_environment_monitoring_network_node.html;jsessionid=412F5EEAFAAC2268952C7E816A1F8791.live11314).

Author contributions

K.S. performed the analysis of the reanalyses and observational data. H.E.M.M. designed the research and wrote the manuscript. K.S. and M.G. contributed with comments, read and approved the manuscript.

Funding

Open Access funding enabled and organized by Projekt DEAL.

Competing interests

The authors declare no competing interests.

Additional information

Supplementary information The online version contains supplementary material available at <https://doi.org/10.1038/s43247-024-01268-z>.

Correspondence and requests for materials should be addressed to H. E. Markus Meier.

Peer review information *Communications Earth & Environment* thanks the anonymous reviewers for their contribution to the peer review of this work. Primary Handling Editors: Regina Rodrigues, Heike Langenberg. A peer review file is available.

Reprints and permissions information is available at <http://www.nature.com/reprints>

Publisher's note Springer Nature remains neutral with regard to jurisdictional claims in published maps and institutional affiliations.

Open Access This article is licensed under a Creative Commons Attribution 4.0 International License, which permits use, sharing, adaptation, distribution and reproduction in any medium or format, as long as you give appropriate credit to the original author(s) and the source, provide a link to the Creative Commons licence, and indicate if changes were made. The images or other third party material in this article are included in the article's Creative Commons licence, unless indicated otherwise in a credit line to the material. If material is not included in the article's Creative Commons licence and your intended use is not permitted by statutory regulation or exceeds the permitted use, you will need to obtain permission directly from the copyright holder. To view a copy of this licence, visit <http://creativecommons.org/licenses/by/4.0/>.

© The Author(s) 2024